Folliculin Controls Lung Alveolar Enlargement and Epithelial Cell Survival through E-cadherin, LKB1 and AMPK

Elena A. Goncharova, Dmitry A. Goncharov, Melane L. James, Elena N. Atochina-Vasserman, Victoria Stepanova, Seung-Beom Hong, Hua Li, Linda Gonzales, Masaya Baba, W. Marston Linehan, Andrew J. Gow, Susan Margulies, Susan Guttentag, Laura S. Schmidt, and Vera P. Krymskaya

Figure S1

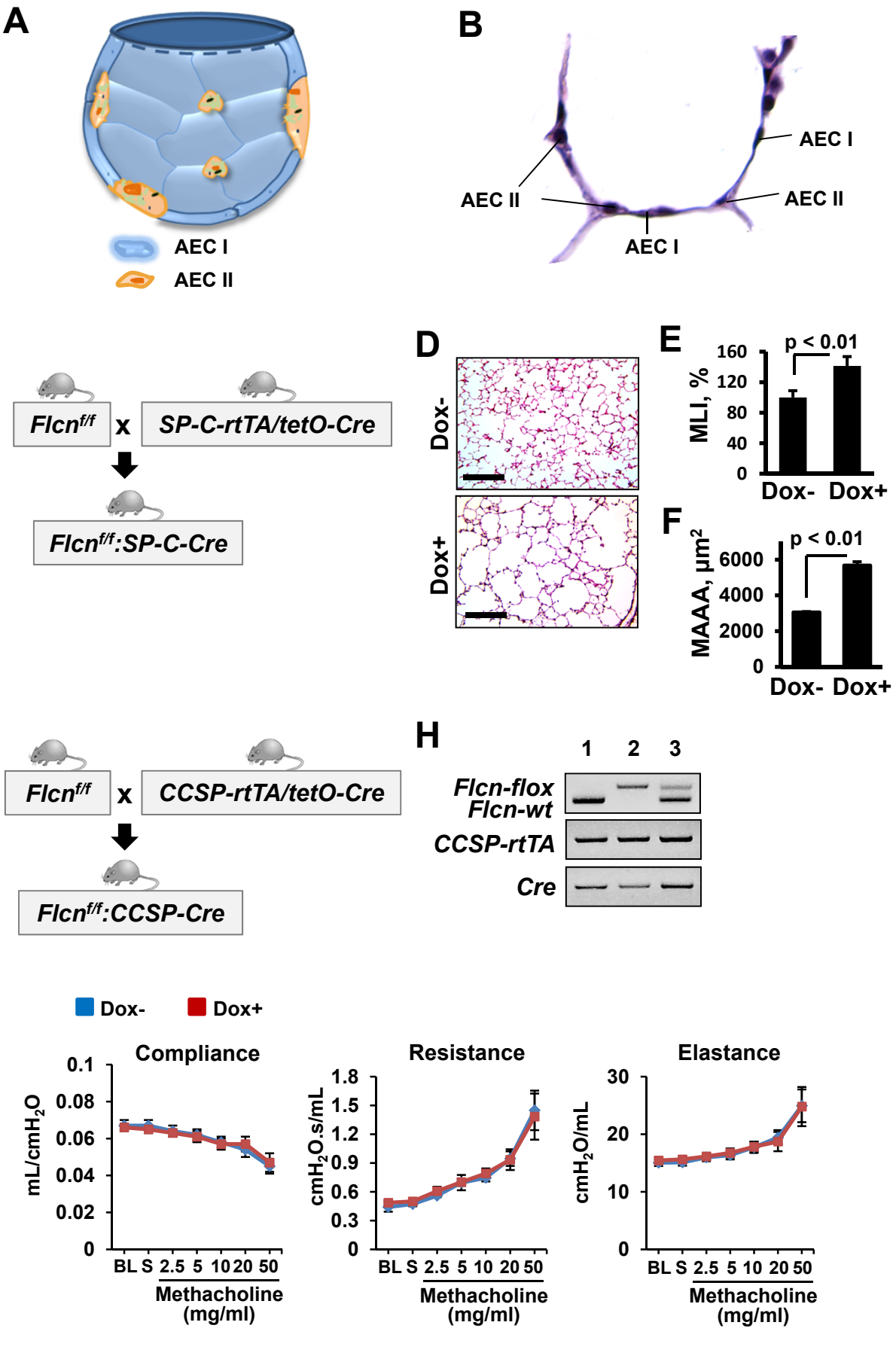
A
AEC I
AEC II
B
AEC I
AEC II
AEC II
AEC I
C
Flcn f/f
x
SP-C-rtTA/tetO-Cre
Flcn f/f:SP-C-Cre
D
Dox-
Dox+
E
p < 0.01
MLI, %
160
120
80
40
0
Dox- Dox+
F
p < 0.01
MAAA, µm2
6000
4000
2000
0
Dox- Dox+
G
Flcn f/f
x
CCSP-rtTA/tetO-Cre
Flcn f/f:CCSP-Cre
H
1 2 3
Flcn-flox
Flcn-wt
CCSP-rtTA
Cre
I
Dox-
Dox+
Compliance
mL/cmH2O
0.1
0.08
0.06
0.04
0.02
0
BL S 2.5 5 10 20 50
Methacholine (mg/ml)
Resistance
cmH2O.s/mL
1.8
1.5
1.2
0.9
0.6
0.3
0
BL S 2.5 5 10 20 50
Methacholine (mg/ml)
Elastance
cmH2O/mL
30
20
10
0
BL S 2.5 5 10 20 50
Methacholine (mg/ml)

Figure S2

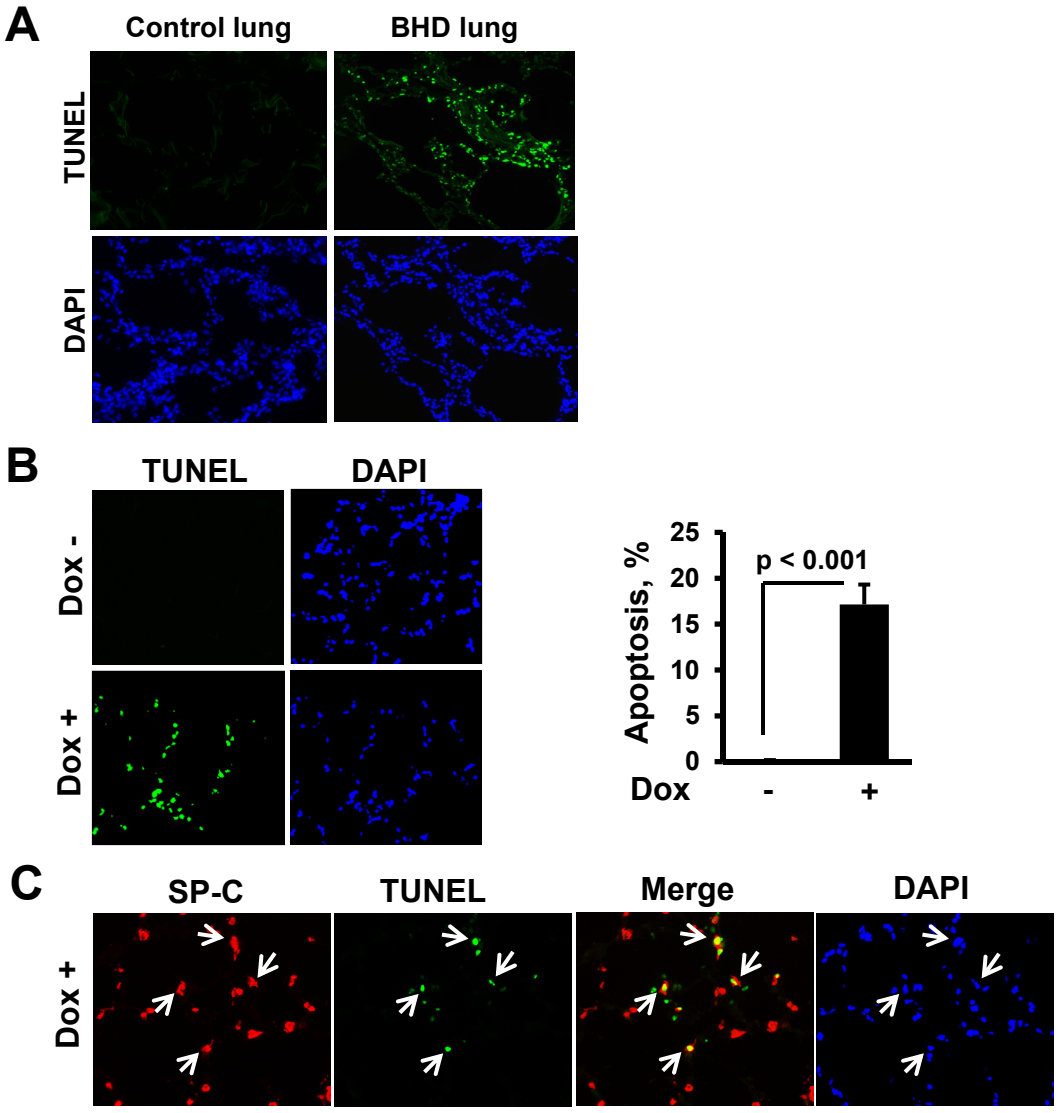
A
Control lung
BHD lung
TUNEL
DAPI
B
TUNEL
DAPI
Dox -
Dox +
Apoptosis, %
25
20
15
10
5
0
p < 0.001
Dox
-
+
C
SP-C
TUNEL
Merge
DAPI
Dox +

Figure S3

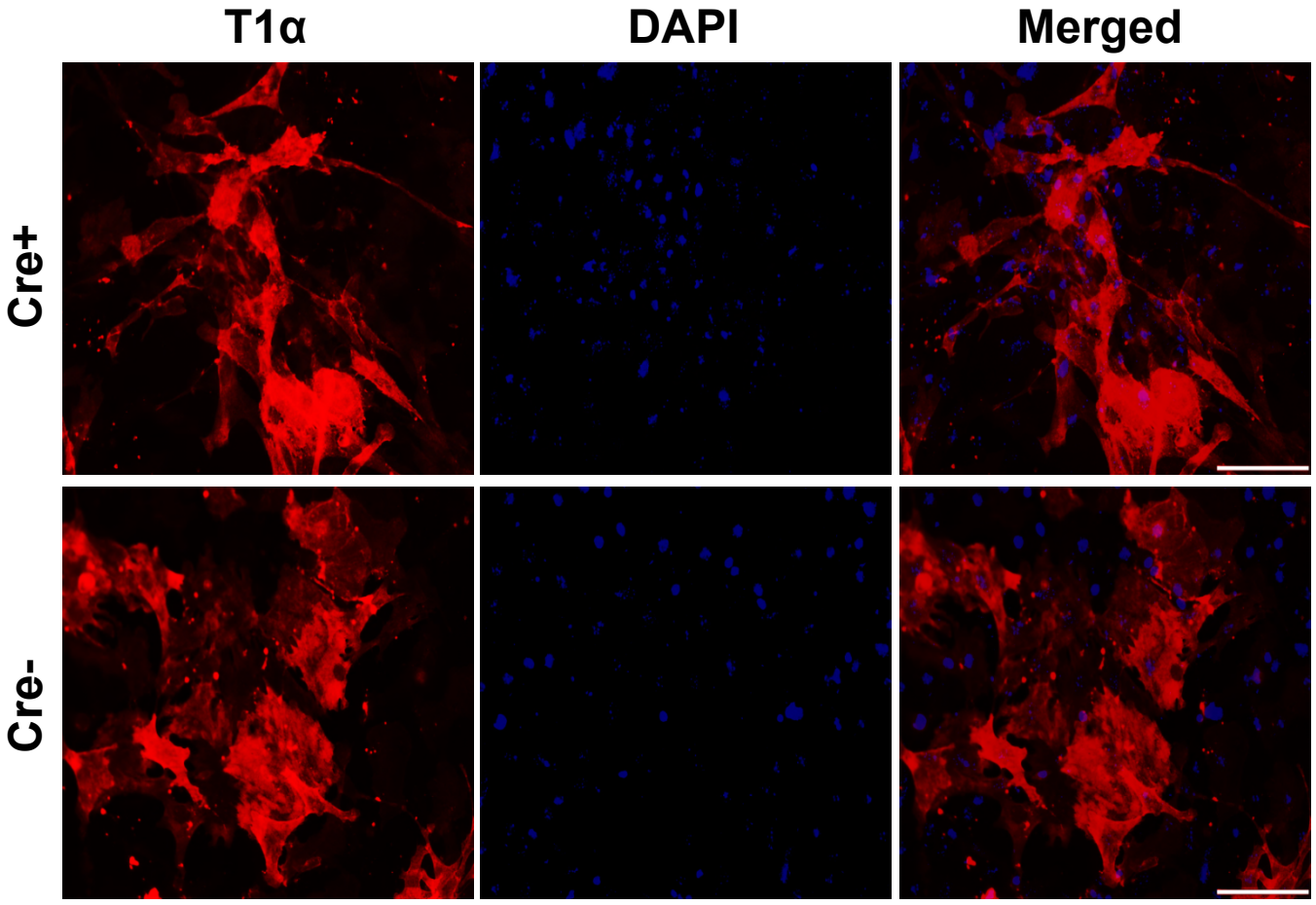

Figure S4

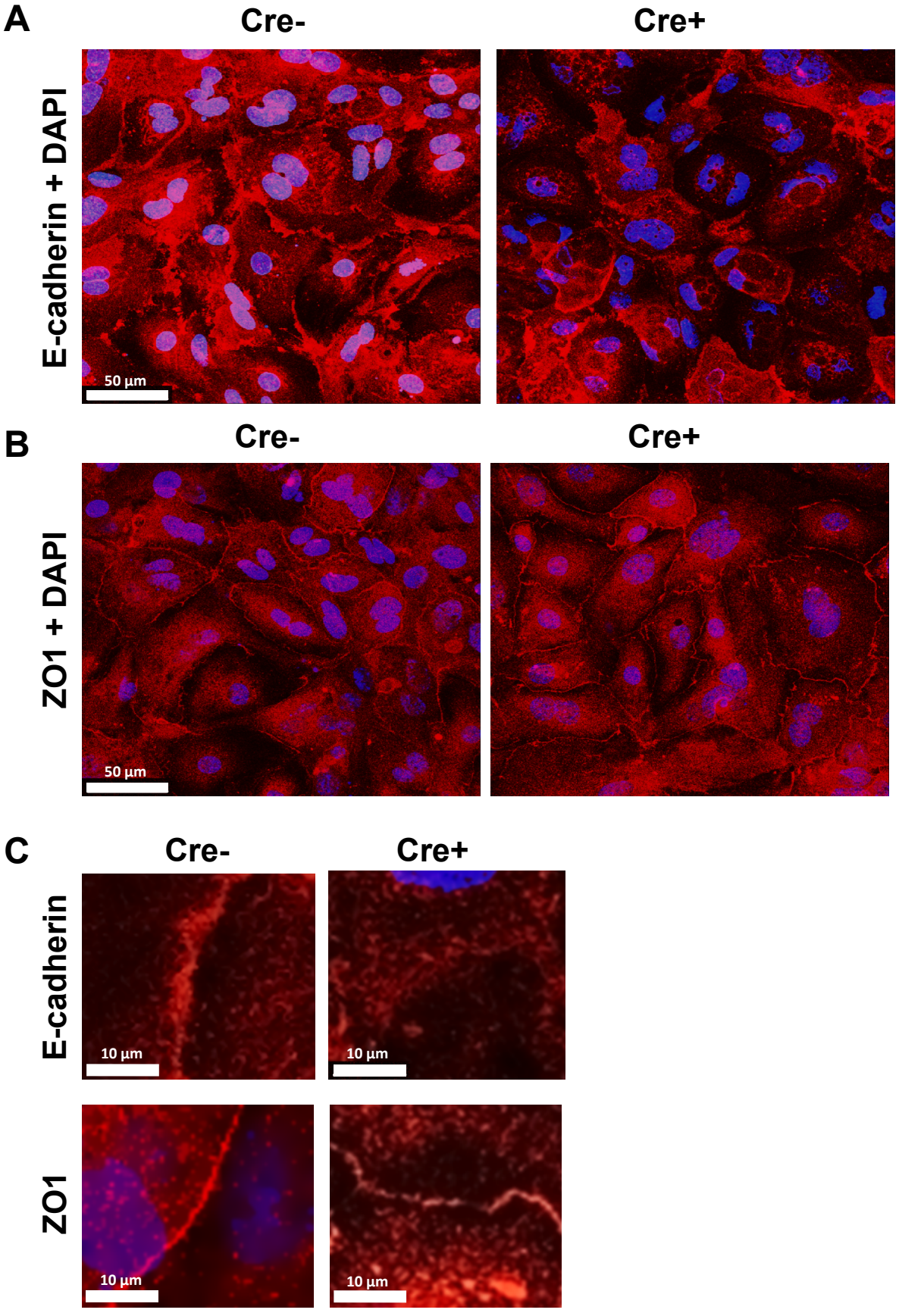
A
Cre-
Cre+
E-cadherin + DAPI
50 µm
B
Cre-
Cre+
ZO1 + DAPI
50 µm
C
Cre-
Cre+
E-cadherin
10 µm
10 µm
ZO1
10 µm
10 µm

Figure S5

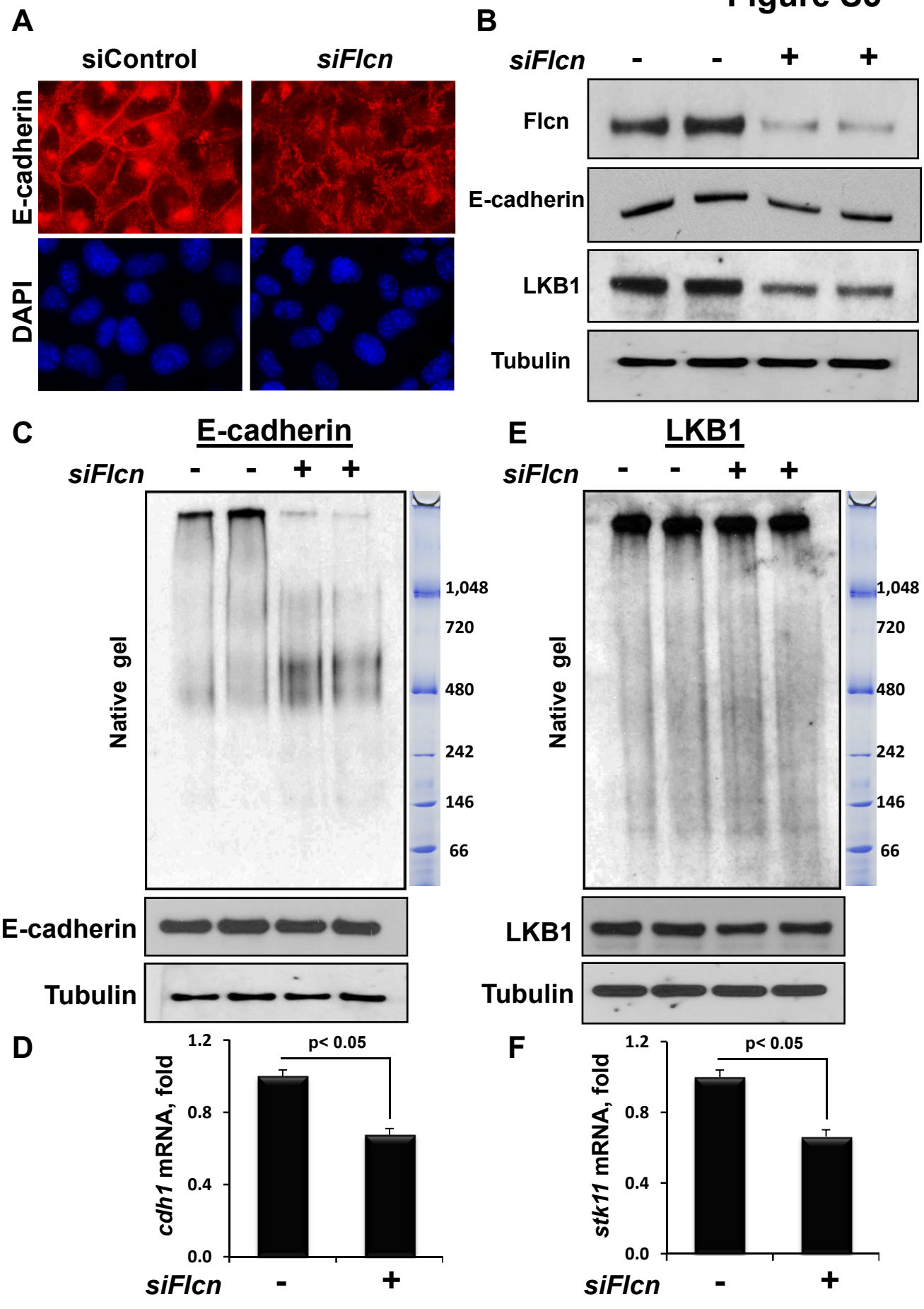
A
siControl
siFlcn
E-cadherin
DAPI
B
siFlcn - - + +
Flcn
E-cadherin
LKB1
Tubulin
C
E-cadherin
siFlcn - - + +
Native gel
1,048
720
480
242
146
66
E-cadherin
Tubulin
E
LKB1
siFlcn - - + +
Native gel
1,048
720
480
242
146
66
LKB1
Tubulin
D
p< 0.05
cdh1 mRNA, fold
1.2
0.8
0.4
0.0
siFlcn - +
F
p< 0.05
stk11 mRNA, fold
1.2
0.8
0.4
0.0
siFlcn - +

Figure S6

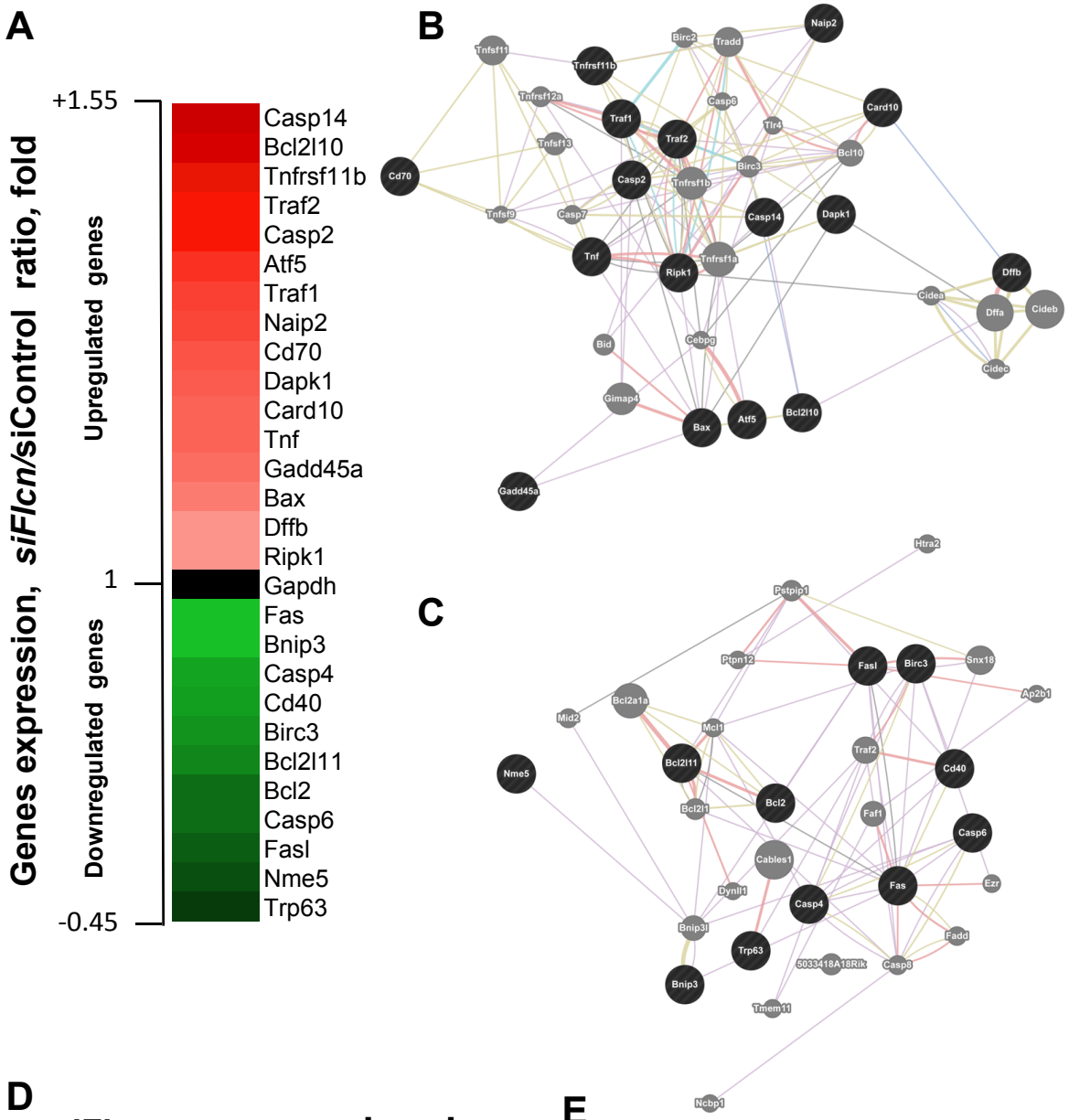
A
Genes expression, siFlcn/siControl ratio, fold
+1.55
1
-0.45
Upregulated genes
Downregulated genes
Casp14
Bcl2l10
Tnfrsf11b
Traf2
Casp2
Atf5
Traf1
Naip2
Cd70
Dapk1
Card10
Tnf
Gadd45a
Bax
Dffb
Ripk1
Gapdh
Fas
Bnip3
Casp4
Cd40
Birc3
Bcl2l11
Bcl2
Casp6
Fasl
Nme5
Trp63
B
C
D
siFlcn - - + +
Bcl-2
Tubulin
Flcn
GAPDH
E
% of siControl
140
120
100
80
60
40
20
0
p< 0.05
p< 0.05
Bcl-2
Flcn

Figure S7

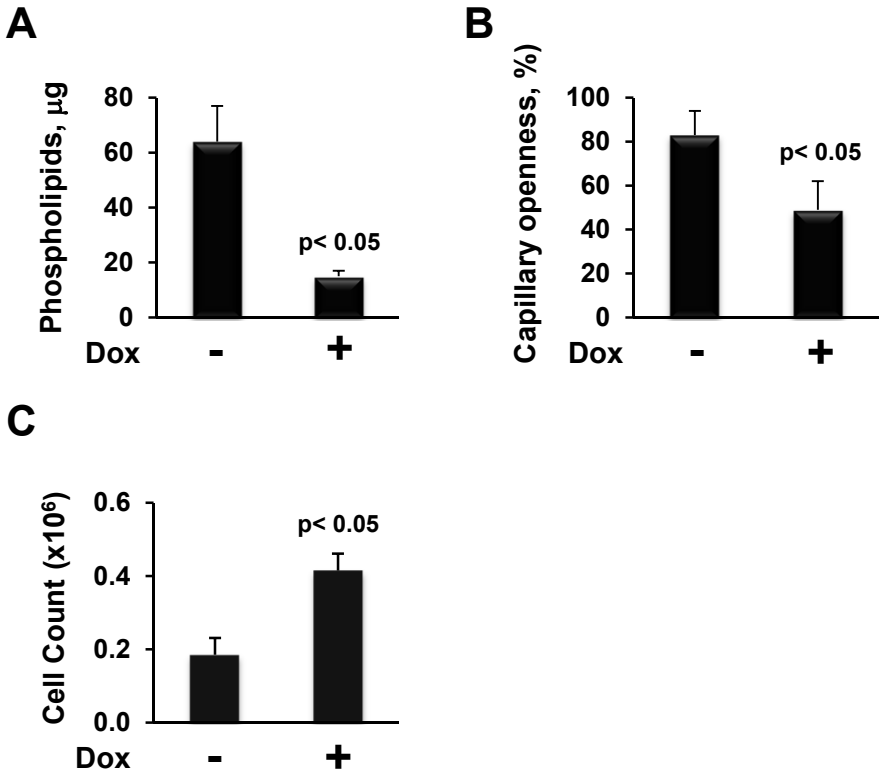
A
Phospholipids, µg
80
60
40
20
0
p< 0.05
Dox
-
+
B
Capillary openness, %)
100
80
60
40
20
0
p< 0.05
Dox
-
+
C
Cell Count (x10⁶)
0.6
0.4
0.2
0.0
p< 0.05
Dox
-
+

Supplemental Figure Legends

Figure S1. Alveolar morphology, structure and lung function.

(A) Schematic representation of alveoli. Alveolar Epithelial Cell type I (AEC I) is represented in blue, and AEC II is shown in orange.

(B) Representative image of H&E staining showing localization of AECs I and AECs II in mouse alveoli.

(C) *Flcn*$^{f/f}$*:SP-C-Cre* mice were generated by crossing *Flcn*$^{f/f}$ mice with *SP-C-rtTA/tetO-Cre* mice (line 2).

(D-F) H&E staining (D), MLI (E) and MAAA (F) analyses of lungs from *Flcn*$^{f/f}$*:SP-C-Cre* mice maintained for 3 weeks on regular (Dox-) or 2.5 % doxycycline (Dox+) -supplemented diet. D: Scale bars, 200 μM. E, F: Data are mean±SE by ANOVA (Fisher PLSD), n≥3 animals/group.

(G) *Flcn*$^{f/f}$*:CCSP-Cre* mice were generated by crossing *Flcn*$^{f/f}$ and *CCSP-rtTA/tetO-Cre* (line 2) mice.

(H) PCR-based genotyping of wild-type *Flcn*$^{wt/wt}$: *CCSP-Cre* (1), homozygous *Flcn*$^{f/f}$*:CCSP-Cre* (2), and heterozygous *Flcn*$^{f/wt}$*:CCSP-Cre* mice (3) with primers detecting *Flcn*, *CCSP-rtTA* and *Cre.*

(I) *Flcn*$^{f/f}$*:CCSP-Cre* mice were placed on regular (Dox-) (n=10; red) or 2.5% doxycycline-supplemented chow (Dox+) (n=10; blue) for 6 weeks followed by lung function test using the FlexiVent system. BL-baseline. S-saline. Data are mean±SE by ANOVA (Fisher PLSD).

Related to Figure 1.

Figure S2. FLCN loss induces DNA fragmentation in human BHD and in mouse lung epithelium deficient for FLCN.

(A) Analysis of tissue specimens from non-diseased (control lung) and BHD patient (BHD lung) to detect apoptotic cells (TUNEL, green) and nuclei (DAPI, blue).

(B) *Flcn*$^{f/f}$*:SP-C-Cre* mice were placed on regular (Dox-) or doxycycline-supplemented diet (Dox+) for 6 weeks followed by lung tissue specimen analysis to detect TUNEL-positive (green) cells. Data are % of TUNEL-positive cells per total number of cells taken as 100%. Data are mean±SE by ANOVA (Fisher PLSD).

(C) Lung tissue from *Flcn*$^{f/f}$*:SP-C-Cre* mice on Dox+ for 6 weeks showing SP-C-positive cells (red), apoptotic cells (TUNEL, green) and DAPI (blue) stained nuclei. Images were taken using Nikon TE-2000E microscope. Arrows indicate cells with co-localization of SP-C and TUNEL (yellow).

Related to Figure 2.

Figure S3. Expression of epithelial cell marker T1α in primary AECs from *Flcn*$^{f/f}$ mice.

Primary AECs isolated from *Flcn*$^{f/f}$ mice were infected with adenovirus expressing Cre-recombinase (Cre+) or control adenovirus (Cre-) for 48 h followed by immunocytochemical analysis to detect T1α (red) and DAPI (blue) staining to detect nuclei. Images were taken using Leica SP5 X Confocal microscope. Scale bars, 100 μM.

Related to Figure 4.

Figure S4. ***Flcn*** **deletion decreases membrane localization of E-cadherin but not ZO1 in primary lung AECs.**

(A) AECs isolated from 2-week-old *Flcn*$^{f/f}$ mice were treated with adenovirus expressing Cre-recombinase (Cre+) or control adenovirus (Cre-) for 48 h followed by immunostaining with E-cadherin (red).

(B) Immunostaining of AECs treated as in (A) with ZO1 antibodies (red).

DAPI staining was performed to detect nuclei (blue). Images were taken on Leica SP5 X confocal microscope. Scale bars, 50 μM.

(C) High resolution of membrane localization of E-cadherin and ZO1 in AECs in enlarged inserts shown in Figure 5D. Scale bars, 10 μM.

Related to Figure 5.

Figure S5. siRNA-induced knockout of FLCN decreases membrane localization, protein and gene expression of E-cadherin in mouse epithelial NMuMG cells.

(A) Mouse epithelial NMuMG cells were transfected with control scrambled siRNA (siControl) or siRNA *Flcn* (*siFlcn*) for 48 hours followed by immunocytochemical analysis with E-cadherin (red) antibody. DAPI staining (blue) shows nuclei. Images were taken on Nikon Eclipse 80i microscope.

(B) Cells transfected as in (A) were lysed followed by immunoblot analysis for Flcn, E-cadherin, LKB1 and tubulin.

(C and E) Flcn loss modulates multimeric structure of E-cadherin. Native electrophoresis (top panels) was performed on cell lysate prepares as in (A) by equal

loading of E-cadherin or LKB1 proteins (top panels). Equal loading of E-cadherin and LKB1 were confirmed by SDS-PAGE analisis of the same cell lysates(bottom panels).

(D and F) Flcn loss downregulates E-cadherin (chd1) and LKB1 (stk1) gene expression. Total mRNA was isolated from cells treated as in (A) followed by RT-qPCR using ABI-prism 7300 sequence detection system (Applied Biosystems). The target genes for E-cadherin (cdh1, Mm01247357_m1), LKB1 (stk11,Mm00488470_m1) and β-actin (Actb, Mm0060793_s1) were amplified by ABI gene assays using the Taqman Univeral PCR master mix (Applied Biosystems). The cycle conditions were set as follows: 95°C for 10 min followed by 40 cycles of 95°C for 15 s and 60°C for 1 min. Each sample was run in triplicates. All data are presented as fold change of cells transfected with *siFlcn* over siControl, calculated by the ΔΔCt method (Livak, 2001) using β-actin as reference gene. Data are expressed as fold change (means ± SEM, n=4; by t-test).

Related to Figure 6.

Figure S6. Loss of FLCN modulates pro-apoptotic gene expression.

(A) Heat map of *Flcn*-dependent gene expression. Mouse epithelial NMuMG cells were transfected as in Figure S5 and the resultant mRNA was analyzed for expression levels of genes involved in regulation of apoptosis (Mouse Apoptosis PCR array, PAMM-012ZA) by RT^2 Profiler PCR Array (SABiosciences, QIAGEN) according to the manufacturer's protocol. The expression of genes was analyzed as in Figure S5D and S5F and presented as fold change *siFlcn* treated over siControl.

(B) The 16 genes with the highest fold increase in expression, shown in red in (A), were analyzed for interaction using the online software Genemania (www.genemania.org).

(C) The 11 genes with the largest reduction in expression, shown in green in (A) were analyzed for interaction as in **B**.

The input genes are shown in black, while predicted interacting genes are shown in grey. Connections are shown as purple for co-expression, pink for physical interaction, blue for known pathway interaction, and green for shared structural domain. The network is centered on interactions between cell survival genes, notably Bcl2 and Fasl.

(D) Flcn loss downregulates pro-survival Bcl-2.

Cells were transfected with control scrambled siRNA (siControl) or siRNA *Flcn* (*siFlcn*) for 48 hours followed by immunoblot analysis with Bcl-2, Flcn and tubulin and GAPDH as the reference gene.

(E) Densitometric quantification of proteins content shown in (D) presented as a percentage of siControl. Values are shown as means + SEM; $p<0.05$ by t-test.

Related to Figure 6.

Figure S7. *Flcn* deletion in lung epithelium of *Flcn*$^{f/f}$*:SP-C-Cre* mice decreases phospholipids and increases surface tension and inflammatory cell infiltrates.

BAL fluid was collected from mice maintained for 2 weeks on regular (Dox-) or doxycycline-supplemented (Dox+) diet and analyzed for

(A) phospholipid level,

(B) surface tension and

(**C**) total cell counts. Data mean ± SEM; by t-test, n = 3-8 samples per group.

Related to Figure 7.

Cited reference:
Livak, K.J. and Thomas D. Schmittgen, T.D. Analysis of Relative Gene Expression Data Using Real-Time Quantitative PCR and the $\Delta\Delta$Ct Method. METHODS **25,** 402–408 (2001). doi:10.1006/meth.2001.1262, available online at http://www.idealibrary.com